ICONHIC2026
4th International Conference on Natural Hazards & Infrastructure
29 June – 2 July 2026, Chania, Greece

Modelling cross-spatial correlation for Sa(T), PGA, PGV, Sa_{avg}(T), and FIV3 for active shallow crustal zones

Vitor A. Monteiro[1], Savvinos Aristeidou[1], and Gerard J. O'Reilly[1]

[1]*Scuola Universitaria Superiore IUSS Pavia, Italy*

ABSTRACT

Spatial correlation of ground motion intensity measures (IMs) is essential in seismic risk assessment, as it governs how shaking varies across sites during an earthquake. While conventional IMs such as *PGA*, *PGV*, and *Sa*(*T*) have established models available in the literature, next-generation IMs like Sa_{avg}(T) and *FIV3* lack spatial and cross-spatial correlation models despite their growing use in engineering applications. In this study, a spatial cross-correlation model for within-event residuals of five IMs was developed, combining conventional and next-generation IMs. The model was derived using principal component analysis (PCA) and geostatistical techniques applied to 11,499 ground motion records from the NGA-West2 and ESM databases. Results show strong agreement with existing models for traditional IMs and fills a key gap for next-generation IMs, enabling more realistic regional risk assessments and supporting their integration into modern hazard and loss frameworks.

Keywords: cross-spatial correlation, intensity measures, regional assessment, seismic risk

INTRODUCTION

Regional-scale seismic risk assessment has been an active area of research since the early 2000s (e.g., Wang & Takada, 2005, Park et al., 2007) and continues to evolve with recent advances (e.g., Bodenmann et al., 2023, Heresi & Miranda, 2023, Acevedo et al., 2025, Bantis et al., 2025). A key objective at this scale is to quantify the spatial distribution of earthquake-induced losses across large building portfolios, which has motivated the development of spatial correlation models for ground motion. Neglecting spatial correlation has been shown to significantly bias regional loss estimated (e.g., Park et al., 2007). Over the past two decades, numerous models have been proposed to describe the spatial correlation of ground motion intensity measures (IMs), as well as their cross-correlation. These include the Markov-type screening hypothesis (e.g., Goda & Hong, 2008), linear model of coregionalization (LMC) (e.g., Loth & Baker, 2013), principal component analysis (PCA) (e.g., Markhvida et al., 2018; Du & Ning, 2021), and latent dimension approaches (e.g., Abbasnejadfard et al., 2020). A recent review by Monteiro & O'Reilly (2026) provides a comprehensive comparison of existing correlation models, IMs, and datasets used in regional risk assessments. In parallel, advances in vulnerability modelling have increased the use of next-generation IMs, such as average spectral acceleration, $Sa_{avg}(T)$, and filtered incremental velocity, $FIV3$. Both IMs have shown improved efficiency, sufficiency, and predictive capability for assessing collapse risk and estimating losses across a broad range of structural systems and ground motion types (e.g.,

[1] PhD Candidate at IUSS Pavia, vitor.azevedomonteiro@iusspavia.it

Eads et al., 2015; Kazantzi & Vamvatsikos, 2015; Davalos & Miranda, 2019; O'Reilly, 2021). However, the development of spatial and cross-spatial correlation models for these IMs has lagged behind, particularly in relation to their interaction with conventional IMs such as $Sa(T)$, PGA, and PGV. This gap limits the use of more informative IMs in regional-scale seismic risk analyses. This study proposes a spatial cross-correlation model for within-event residuals across both conventional and next-generation IMs. The model was developed using PCA and geostatistical tools and is calibrated using a combined dataset of 11,499 ground motion records from the NGA-W2 (Ancheta et al., 2014) and European strong motion (ESM) databases (Lanzano et al., 2019). An illustrative example demonstrates the generation of ground motion fields for next-generation IMs, highlighting the applicability of the proposed model in scenario-based seismic risk assessment.

GROUND MOTIONS

Available datasets

Several extensive ground motion datasets have played a critical role in developing spatial correlation models. Commonly employed datasets include Japan's K-NET and KiK-net networks (Aoi et al., 2004), the RESORCE database (Akkar et al., 2014), ITACA (Luzi et al., 2008), and the Ridgecrest database (Rekoske et al., 2020). Although each of these could have been suitable for this study, two major databases were selected: the NGA database compiled by Ancheta et al. (2014) and the ESM database curated by Lanzano et al. (2019). These datasets were used to develop a global cross-IM spatial correlation model for active shallow crustal regions. Here, the term *cross-IM* indicates that the model establishes correlations between different IMs. A total of 81 earthquakes were selected from the combined NGA-W2 and ESM datasets. The databases were filtered based on the same criteria outlined in Aristeidou et al. (2024), resulting in 11,499 records, where 7,728 arose from NGA-W2 and 3,771 from ESM.

Intensity Measures

Several IMs are used in seismic engineering depending on the structural typology and analysis objectives. The IMs considered in the cross-IM spatial correlation modelling in this study include:

- PGA: peak ground acceleration;
- PGV: peak ground velocity;
- $Sa(T)$: 5% damped spectral acceleration at a vibration period, T, where $T \in [0.01, 0.05, 0.075, 0.1, 0.2, 0.3, 0.4, 0.5, 0.75, 1.0, 1.5, 2.0, 3.0, 4.0, 5.0]$s;
- $Sa_{avg}(T)$: average spectral acceleration, defined as the geometric mean of 10 linearly-spaced spectral acceleration values over two different period ranges from $0.2T$ to $2.0T$ and $0.2T$ to $3.0T$, which were termed (Shahnazaryan & O'Reilly, 2024) $Sa_{avg2}(T)$: and $Sa_{avg3}(T)$:, respectively, where $T \in [0.1, 0.15, 0.20, 0.30, 0.40, 0.50, 0.60, 0.75, 0.8, 0.9, 1.0, 1.2, 1.5, 2.0, 2.5, 3.0, 4.0]$s;
- $FIV3$ defined by Davalos et al, (2019) and following their recommendation, values of $\alpha = 0.7$ and $\beta = T$ were adopted for the calculation of the IMs, where $T \in [0.1, 0.15, 0.20, 0.30, 0.40, 0.50, 0.60, 0.75, 0.8, 0.9, 1.0, 1.2, 1.5, 2.0, 2.5, 3.0, 4.0]$s.

Ground motion models and residuals

The IMs values and corresponding residuals were computed using the generalized ground motion model (GGMM) proposed by Aristeidou et al, (2024). Similar to other GMMs developed in the past, this model adopts the conventional lognormal functional form expressed as:

$$log_{10} IM_{i,k,m} = \mu_i\left(X_{k,m}, \theta\right) + \delta b_{i,k} \cdot \tau_i + \delta w_{i,k,m} \cdot \phi_i \quad (1)$$

where $log_{10} IM_{i,k,m}$ is the logarithm of i^{th} IM of interest, $\mu_i\left(X_{k,m}, \theta\right)$ is the predicted mean obtained from the GGMM based on explanatory variables $X_{k,m}$ (e.g., moment magnitude, M_w, rupture

distance, R_{jb}, site conditions, V_{s30}, etc.), and model parameters, θ for a given earthquake k at site m, $\delta b_{i,k}$ and $\delta w_{i,k,m}$ are the normalised between- and within-event residuals of IM_i, respectively, and finally τ_i and ϕ_i are the between- and within-event logarithmic standard deviations, respectively. In spatial correlation models, normalised within-event residuals are utilised, so the formulation to calculate them can be deduced from Equation (1), solving for $\delta w_{i,k,m}$ as:

$$\delta w_{i,k,m} = \frac{log_{10} IM_{i,k,m} - \mu_i(X_{k,m}, \theta) - \delta b_{i,k} \cdot \tau_i}{\phi_i} \quad (2)$$

Previous studies have shown that normalised residuals are well represented by a normal distribution, with noticeable deviations only beyond approximately four standard deviations Baker et al, (2021). Furthermore, IM residuals at multiple sites are commonly modelled as following a multivariate normal distribution with mean zero and an associated covariance structure Jayaram and Baker, (2008).

SPATIAL CORRELATION MODEL DEVELOPMENT

In this section, the theoretical basis to develop a spatial correlation model is first presented using normalised within-event residuals for each IM mentioned before. The approach then follows the PCA-based methodology initially employed by Markhvida et al, (2018), combining PCA and geo-statistical methods to develop the proposed spatial correlation model. Table 1 summarises the cross-IM spatial correlation models developed in this study, denoted as MAO26, and also some other cross-IM spatial correlation models from the literature.

***Table 1**. Cross-IM spatial correlation models proposed here and existing ones from the literature.*

IMs	*Sa(T)*	*Sa$_{avg2}$(T)*	*Sa$_{avg3}$(T)*	*PGA*	*PGV*	*FIV3*
Sa(T)	MAO26 LB13 MCB18 DN21	MAO26	MAO26	MAO26 DN21	MAO26 DN21	MAO26
Sa$_{avg2}$(T)		MAO26	MAO26	MAO26	MAO26	MAO26
Sa$_{avg3}$(T)			MAO26	MAO26	MAO26	MAO26
PGA				MAO26 DN21	MAO26 DN21	MAO26
PGV					MAO26 DN21	MAO26
FIV3						MAO26

MAO26: This study; LB13: Loth & Baker, 2013; MC18: Markhvida et al. 2018; DN21: Du & Ning, 2021.

Spatial correlation using principal components

Empirical semivariograms and cross-semivariograms were computed for each transformed dataset using a distance bin of 2km. For each model and each principal component (PC), the pooled data across all stations was used, resulting in a total of 1,279,694 station pairs. To characterise the spatial dependence structure of the PCs, a nested semivariogram model proposed by Markhvida et al, (2018) was employed. This model, presented in Equation (3) accounts for the initial discontinuity at the origin, commonly referred to as the nugget effect, as well as both short-range and long-range spatial correlation behaviours. In this formulation, $\xi_{h=0}$

is an indicator function that takes the value of 1 when $h = 0$, and 0 otherwise. The parameters c_{0k}, c_{1k}, c_{2k}, a_{1k}, and a_{2k} are regression coefficients estimated for each principal component k.

$$\gamma(k) = c_{0k}(1 - \xi_{h=0}) + c_{1k}\left(1 - exp\left(\frac{-3h}{a_{1k}}\right)\right) + c_{2k}\left(1 - exp\left(\frac{-3h}{a_{2k}}\right)\right) \quad (3)$$

Figure 1 illustrates the empirical semivariograms and the corresponding fitted nested models for the first five principal components, shown for two representative cases. Figure 1(a) corresponds to the model $Sa(T) - Sa(T)$, while Figure 1(b) shows results for the model $Sa_{avg2}(T) - FIV3(T)$. As observed in both figures, the spatial correlation structure varies considerably with PC order. In this context, it's useful to identify how many PCs of the transformed data are necessary to retain a significant amount of the original variance, since the first PC captures most of the variance, and so on. In many cases, particularly for higher-order components, the empirical semivariance increases only gradually with distance, which would justify the use of a simplified model that accounts only for the nugget effect. Nevertheless, for consistency across the 21 models developed, the nested structure was retained and fitted to all PCs in all models.

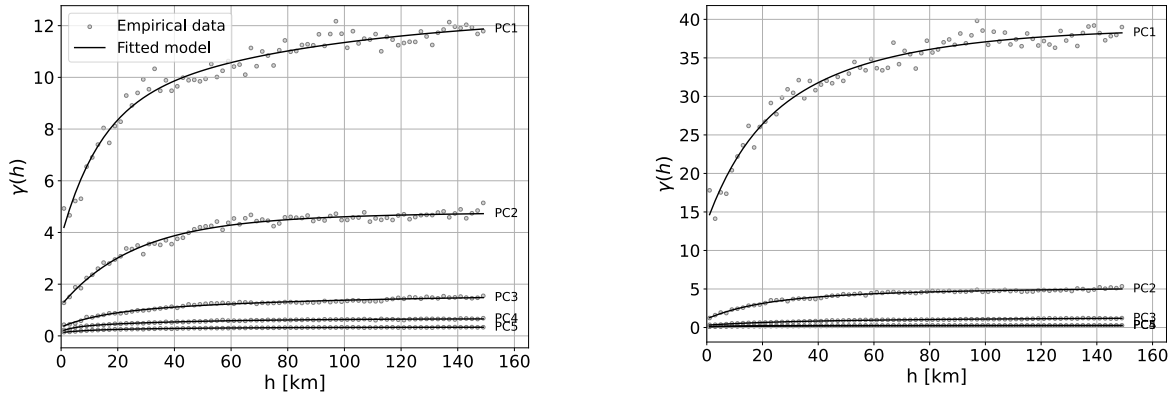

Figure 1. *Empirical semivariograms and the fitted models for the first 5 principal components (PCs) of (a)* $Sa(T) - Sa(T)$ *and (b)* $Sa_{avg2}(T) - FIV3(T)$.

RESULTS

Model fitting

To validate the proposed models, it was essential to compare the spatial variability derived from empirical ground motion residuals in the original normalised space with the modelled cross-semivariograms, which relies on a multivariate adaptation of the covariance structure to incorporate inter-IM relationships. Following the formulation by Markhvida et al, (2018), the cross-semivariogram between two IMs, IM_i and IM_j, can be written as:

$$\gamma_{IM_i,IM_j}(h) = C_{IM_i,IM_j}(0) - C_{IM_i,IM_j}(h) \quad (4)$$

$$= \sum_{K=1}^{N} p_{k,IM_i} p_{k,IM_i} COV\big(Y_k(x), Y_k(x)\big) - \sum_{K=1}^{N} p_{k,IM_j} p_{k,IM_j} COV\big(Y_k(x), Y_k(x+h)\big)$$

$$= \sum_{K=1}^{N} p_{k,IM_i} p_{k,IM_j} \big(C_k(0) - C_k(h)\big)$$

$$= \sum_{K=1}^{N} p_{k,IM_i} p_{k,IM_j} \gamma_k(h)$$

Here, p_{k,IM_i} and p_{k,IM_j} are the coefficients of the k^{th} PC for the respective IMs, obtained from the PCA transformation matrix P, and N is the total number of principal components used. The term $\gamma_k(h)$ represents the semivariogram of the k^{th} PC evaluated at separation distance h, calculated using Equation (3). This decomposition enables the reconstruction of the cross-semivariogram

in the original space as a weighted sum of individual PC semivariograms. Empirical semivariograms and cross-semivariograms are estimated using the residuals of the original IMs. By comparing these empirical estimates with the model-based reconstructions, it is possible to assess how well the PCA-based approach captures the spatial correlation structure across different IMs. The semivariogram, variance, and covariance functions must be normalised by the explained variance percentage to account for the missing variance. This normalisation was applied by Markhvida et al., (2018) and Du & Ning, (2021) as shown in Equations (5), (6), and (7), respectively.

$$\gamma(k) = \frac{c_{0k}(1-\xi_{h=0}) + c_{1k}\left(1 - exp\left(\frac{-3h}{a_{1k}}\right)\right) + c_{2k}\left(1 - exp\left(\frac{-3h}{a_{2k}}\right)\right)}{\%\sigma_{expl.cum}{}^2} \tag{5}$$

$$C_k(h) = \frac{c_{0k} + c_{1k} + c_{2k}}{\%\sigma_{expl.cum}{}^2} \tag{6}$$

$$\begin{aligned} C_k(h) &= C_k(0) - \gamma(k) \\ &= \frac{c_{0k}(\xi_{h=0}) + c_{1k}\left(exp\left(\frac{-3h}{a_{1k}}\right)\right) + c_{2k}\left(exp\left(\frac{-3h}{a_{2k}}\right)\right)}{\%\sigma_{expl.cum}{}^2} \end{aligned} \tag{7}$$

The cross-variance and cross-covariance for each pair of IMs can be computed with the same methodology as Equation (4), as shown in Equations (8) and (9), respectively. The final correlation, $\rho_{IM_i,IM_j}(h)$, is then obtained as per Markhvida et al., (2018).

$$C_{IM_i,IM_j}(0) = \sum_{k=1}^{N} p_{k,IM_i} p_{k,IM_j} C_k(0) \tag{8}$$

$$C_{IM_i,IM_j}(h) = \sum_{k=1}^{N} p_{k,IM_i} p_{k,IM_j} C_k(h) \tag{9}$$

To understand how the fitted semivariograms and cross-semivariograms compared to the empirical values, Figure 2 presents examples of these comparisons for different IM pairs. Each plot shows both empirical and modelled semivariograms and cross-semivariograms using all selected PCs in the summation. The results indicate that while the PCA-based model generally preserves spatial correlation patterns across different IM types, including $Sa(T)$, $Sa_{avg}(T)$, and other measures like $FIV3(T)$, some deviations are observed. In particular, pairs like $FIV3(T) - Sa(T^*)/Sa_{avg}(T^*)$, and $PGV - Sa(T^*)/Sa_{avg}(T^*)$, for $T^* \lesssim 1s$, show less accurate fitting, which will be explored further in the next section.

Generalised versus piecewise fitting of PCs

The imperfect fitting observed in Figure 2 for some IM pairs was already observed in Markhvida et al. (2018) and Du & Ning (2021), which suggests that the full PCA-based models, which incorporates many IMs simultaneously, sometimes fail to capture pairwise spatial correlations accurately. This is because including multiple IMs compromises the fitting accuracy of specific pairs whilst trying to maintain overall accuracy. To address this, a simplified modelling approach that focuses on each pair of IMs individually was investigated, using only two principal components relevant to that pair and one PC in the case of using the same IM.

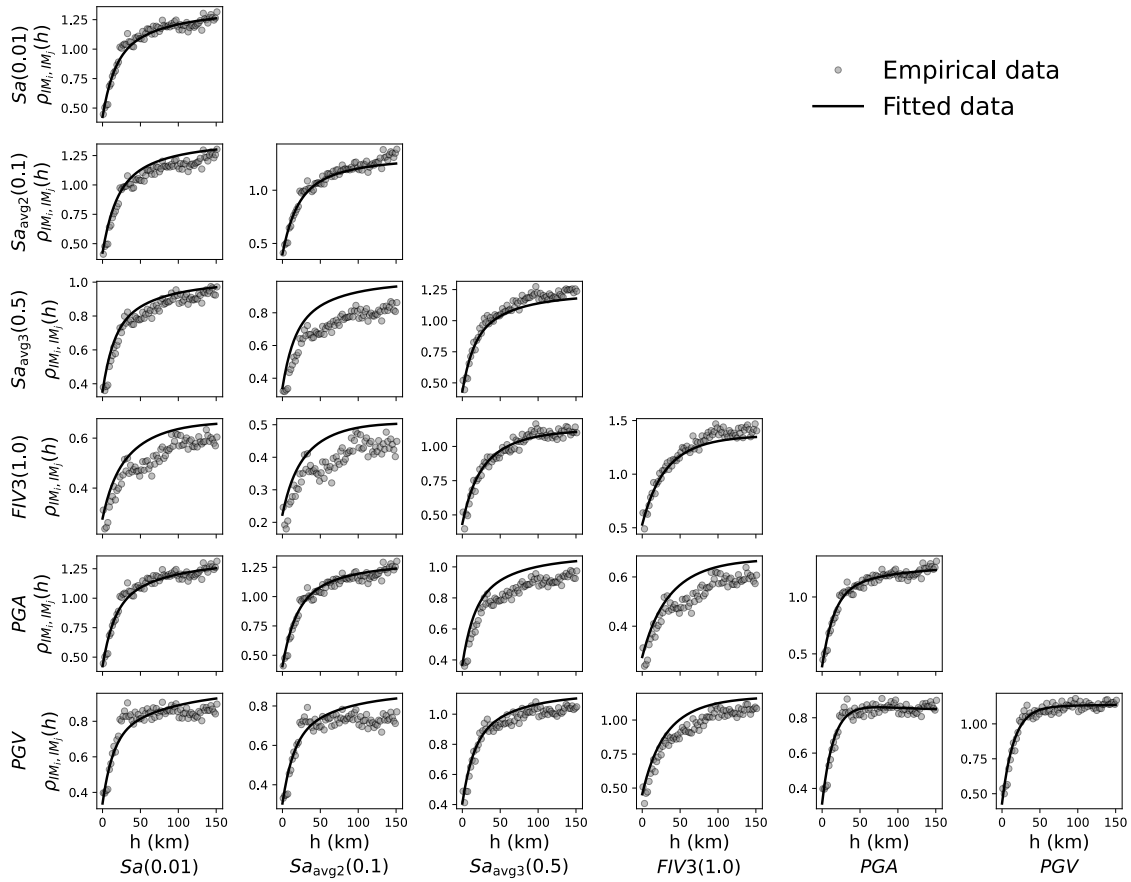

***Figure 2**. Comparison between empirical semivariogram and model semivariogram using Equation (4) with all principal components for the model used.*

***Table 2**. Comparison of the number of principal components used in the simplified models between this study and models developed by Markhvida et al., (2018) and Du & Ning, (2021).*

Models	This study	Markhvida et al., 2018	Du & Ning 2021
N° of earthquakes	81	45	28
N° of ground motions	11499	4910	3797
N° of PCs used in total	2/1*	19	23
N° of PCs used in reduced model	2/1*	5	7
$\%\sigma^2{}_{expl.cum}$	100	95	90

Instead of reconstructing, for example, $Sa(0.1) - Sa(0.4)$ cross-correlation from a generalised model with 15 PCs covering all $Sa(T)$ periods, each pair was modelled with just two PCs specifically capturing their joint behaviour. Figure 3(a) illustrates this approach with the example of $Sa_{avg2}(0.1) - Sa_{avg2}(1.5)$, where the full model uses 17 PCs, while the simplified use only 2 PCs. The simplified model demonstrates a much-improved fit to the empirical semivariograms, with no real computational penalty, aside from needing to fit several individual models rather than a single one. Applying this simplified modelling approach, where each IM pair is analysed individually, Figure 3(b) presents an example illustration of the difference in weighted least squares (WLS) errors for pair $Sa_{avg2}(T) - Sa_{avg2}(T)$. In this context, the WLS quantifies the discrepancy between the empirical and the modelled semivariograms for $Sa_{avg2}(T)$ obtained using Equation (4). As expected, the simplified two-IM model often yields lower WLS errors, indicating a better fit to the observed spatial variability. For similar plots for other IM-pair cases, these are

available on the GitHub repository: https://github.com/vitorazevedomonteiro/cross-spatial-correlation-model

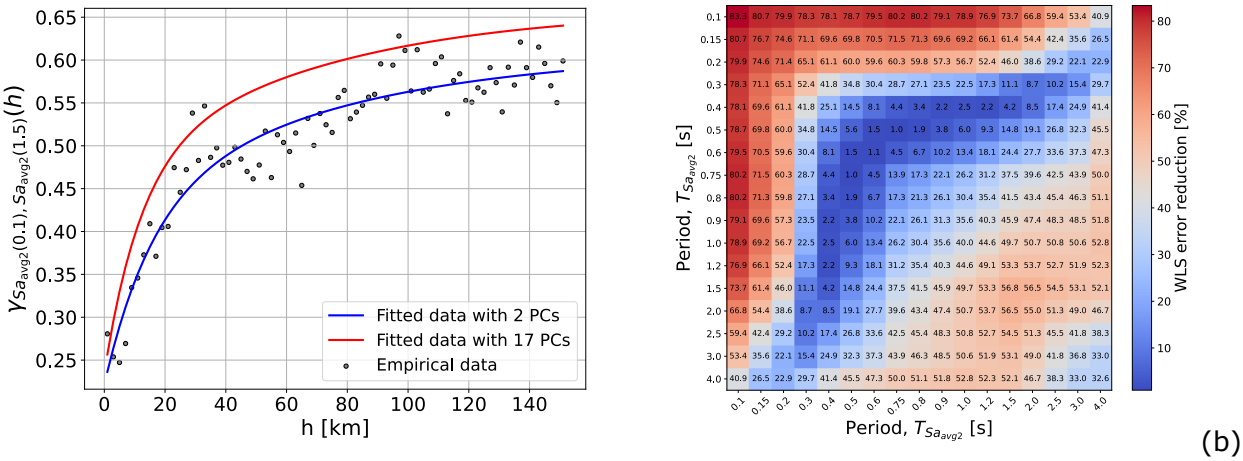

(a) (b)

***Figure 3**. (a) Comparison between PCA-based models with fewer and total amount of principal components for $Sa_{avg2}(0.1) - Sa_{avg2}(1.5)$, cross-semivariogram model, and (b) error reduction for $Sa_{avg2}(T)$ semivariograms and cross-semivariograms when used 2 specific IM pairs and all of the IM pairs simultaneously.*

Comparison with previous models

The performance of the proposed inter-IM spatial correlation model is compared against previous studies that developed cross-spatial correlation models for several IMs as mentioned in Table 1. Figure 4 presents correlograms (plots of correlation coefficients as a function of separation distance) and cross-correlograms for $Sa(T)$ at periods of 0.01, 0.1, 0.5, 1, 2, and 5 seconds. The proposed model exhibits trends generally consistent with those of existing models. Notably, the model by Du & Ning (2021) yields higher correlation values across all periods and distances compared to the other models. In contrast, the proposed model shows a faster decay of spatial correlation with distance than the model by Markhvida et al. (2018), but still generally predicts higher correlations than the model by Loth & Baker (2013). Differences observed among the correlograms and cross-correlograms in Figure 4 can be attributed to several factors, including the choice of ground motion databases and utilised subsets, the number of principal components used in dimensionality reduction, functional forms adopted for the correlation structure, and methodological differences, particularly in the case of Loth & Baker (2013). Further comparison is made for other IMs, including $Sa_{avg2}(T)$, $Sa_{avg3}(T)$, and $FIV3$, as shown in Figure 5. To the authors' knowledge, no direct inter-IM spatial correlation models exist for $Sa_{avg}(T)$ or $FIV3$. In this study, an indirect estimation of $Sa_{avg2}(T)$ correlations were derived following the methodology proposed by Heresi & Miranda (2021) and compared with the direct model proposed herein, showing good overall agreement between both approaches, which has also been discussed in Monteiro and O'Reilly (2026). The presented model offers the first insight into the spatial correlation structure of these composite IMs. With respect to $FIV3$, Aristeidou et al., (2025) observed strong internal correlations of the IM with itself across different periods. In particular, the spatial correlation analysis revealed that the cross-correlograms both across different $FIV3$, periods and between $FIV3$, and PGV, exhibit highly consistent behaviour.

APPLICATION EXAMPLE

To illustrate the application of the proposed spatial cross-correlation model, conditional GMFs were generated for the 1994 Northridge earthquake ($M_w = 6.7$) using the OpenQuake engine (Pagani et al., 2014). For demonstration purposes, four IMs were considered: $Sa(1.0)$, PGV, $Sa_{avg2}(1.0)$, and $FIV3(0.5)$. The resulting GMFs represent expected ground motion fields, obtained

as the logarithmic mean across 10,000 simulations, and were computed using the spatial correlation model developed in this study. Due to the lack of between-event correlation models between IMs other than $Sa(T)$, the GMFs presented here correspond to single-IM conditional fields rather than fully cross-IM simulations. As shown in Figure 6, the simulated GMFs are broadly consistent with the observed values at recording stations. This example underscores the relevance of incorporating realistic spatial correlation models in regional risk assessments. The main advantage of the proposed model is that it allows the consideration of several next-generation IMs, which have been shown to have lower variability when estimating consequences such as economic loss and damage states of structures, which ultimately leads to much more accurate risk assessments.

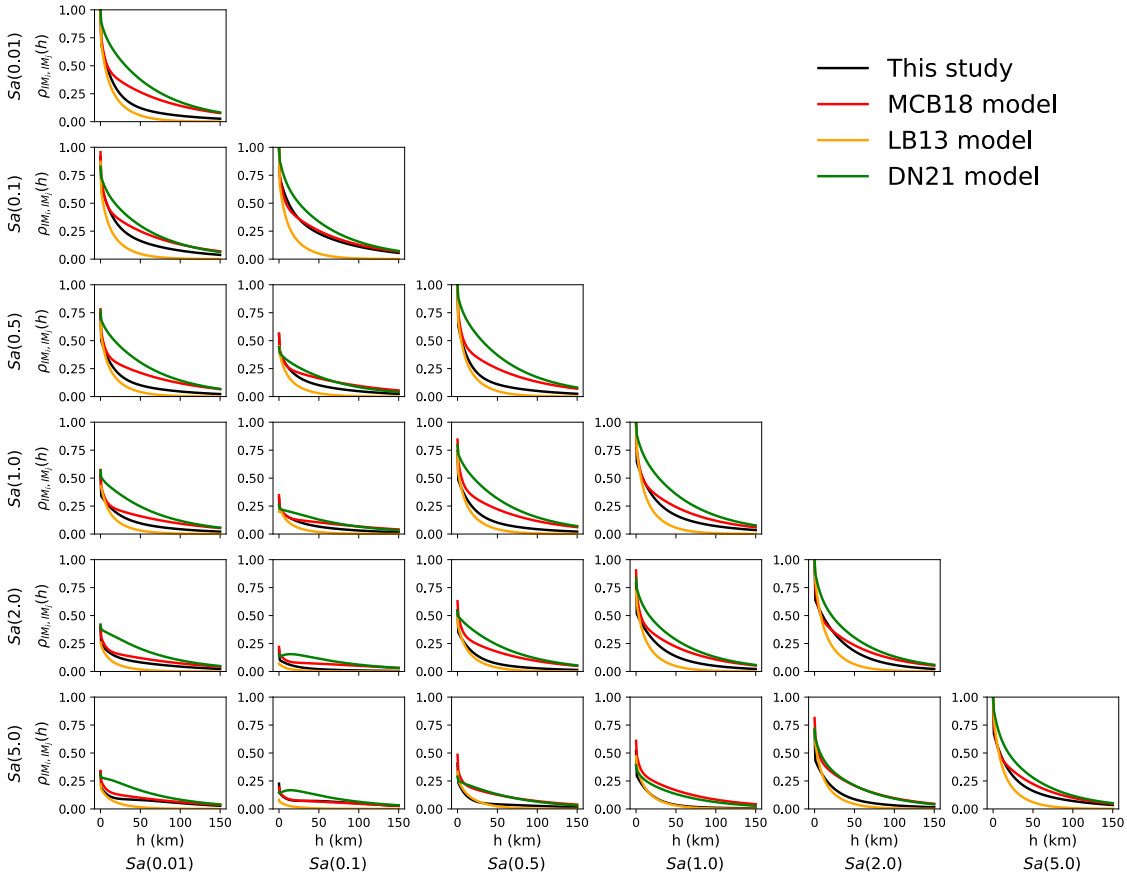

Figure 4. Comparison of the proposed correlograms and cross-correlograms for different $Sa(T)$ between this study and other studies.

SUMMARY AND CONCLUSIONS

This paper presents a new spatial cross-correlation model for several IMs, developed using PCA and geostatistical tools, tailored for active shallow crustal tectonic regions. The model is based on over 11,000 ground motion recordings from two combined databases, NGA-West2 and ESM. It provides spatial coefficients for traditional IMs such as $Sa(T)$, PGA, and PGV, as well as next-generation IMs like $Sa_{avg}(T)$ and $FIV3(T)$. The framework follows the methodology proposed by Markhvida et al. (2018), using PCA to transform spatially correlated normalised within-event residuals into uncorrelated principal components. A key distinction of this study lies in the number of IMs used for the PCA methodology: only two were retained in the models, compared to 19 and 23 in similar prior studies (Markhvida et al., 2018; Du & Ning, 2021, respectively), showing a considerable reduction in the fitting error. This reduction improved model efficiency and provided a better fit across the selected IM-pairs. To validate the proposed model, comparisons were made with existing spatial cross-correlation models, showing strong agreement for common IMs and filling a gap for next-generation IMs such as $Sa_{avg}(T)$ and $FIV3(T)$, for which no prior models currently exist. Finally, an illustrative example demonstrated

the application of the proposed model to generate ground motion fields for $Sa(1.0)$, $Sa_{avg}(1.0)$, PGV, and $FIV3(0.5)$.

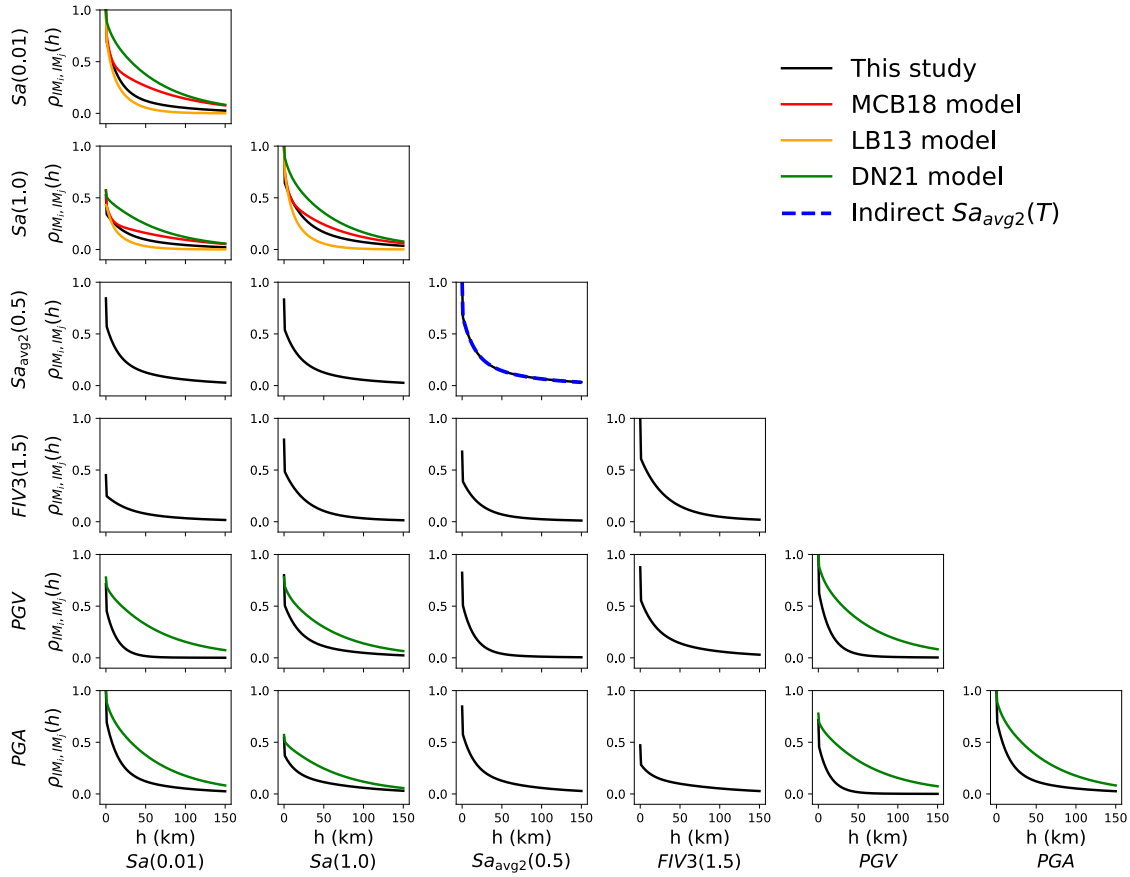

***Figure 5**. Comparison of predicted correlations and cross-correlations for $Sa(T)$, $Sa_{avg2}(T)$, $FIV3$, PGV and PGA between this study and other studies.*

This study highlighted the importance of accurate spatial correlation modelling for realistic scenario simulations in regional risk assessments. While the model assumed stationarity and isotropy, it remains applicable for regional-scale assessments and offers a simpler alternative to more complex frameworks that explicitly incorporate path and site effects (e.g., Bodenmann et al., 2023). However, the proposed approach does not explicitly account for site-specific effects, such as local soil conditions, and therefore its direct application to site-specific earthquakes studies may require additional calibration. Future work should investigate the integration of site-dependent variability and the extension of the framework to site-specific hazard and risk analyses. By addressing a critical gap in current practice (i.e., the lack of reliable spatial correlation structures for next-generation IMs), the proposed model enables more accurate assessments of seismic risk at regional scales. This advancement facilitates the adoption of modern ground-motion metrics into large-scale hazard and loss frameworks, which was the primary motivation of this research.

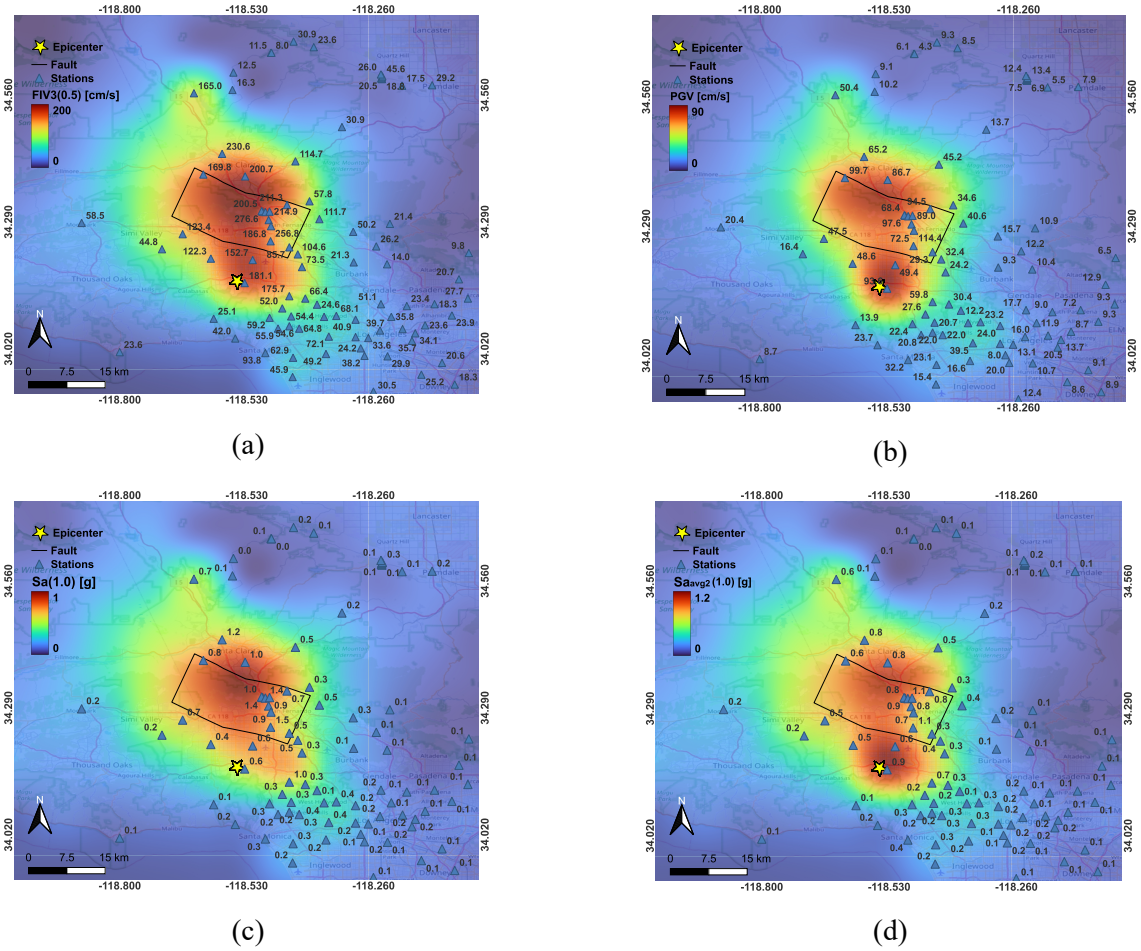

Figure 6. *Conditional ground motion fields for the 1994 Northridge earthquake using the spatial correlation model developed in this study for (a)* $FIV3(0.5)$*, (b)* PGV*, (c)* $Sa(1.0)$*, and (d)* $Sa_{avg2}(1.0)$*.*

REFERENCES

A. B. Acevedo, S. Carrascal, J. F. Betancur, and D. González, "Influence of the spatial distribution of hazard and exposure models on urban seismic risk assessment," *Earthquake Spectra*, June 2025, doi: 10.1177/87552930251341362.

A. K. Kazantzi and D. Vamvatsikos, "Intensity measure selection for vulnerability studies of building classes," *Earthq Eng Struct Dyn*, vol. 44, no. 15, pp. 2677–2694, Dec. 2015, doi: 10.1002/eqe.2603.

C. Loth and J. W. Baker, "A spatial cross-correlation model of spectral accelerations at multiple periods," *Earthq Eng Struct Dyn*, vol. 42, no. 3, pp. 397–417, Mar. 2013, doi: 10.1002/eqe.2212.

D. Shahnazaryan and G. J. O'Reilly, "Next-generation non-linear and collapse prediction models for short- to long-period systems via machine learning methods," *Eng Struct*, vol. 306, p. 117801, May 2024, doi: 10.1016/j.engstruct.2024.117801.

G. J. O'Reilly, "Limitations of Sa(T1) as an intensity measure when assessing non-ductile infilled RC frame structures," *Bulletin of Earthquake Engineering*, vol. 19, no. 6, pp. 2389–2417, Apr. 2021, doi: 10.1007/s10518-021-01071-7.

G. Lanzano *et al.*, "The pan-European Engineering Strong Motion (ESM) flatfile: compilation criteria and data statistics," *Bulletin of Earthquake Engineering*, vol. 17, no. 2, pp. 561–582, Feb. 2019, doi: 10.1007/s10518-018-0480-z.

J. Bantis, P. Heresi, A. Poulos, and E. Miranda, "Framework for Regional Seismic Risk Assessments of Groups of Tall Buildings," *Earthq Eng Struct Dyn*, vol. 54, no. 3, pp. 833–850, Mar. 2025, doi: 10.1002/eqe.4283.

J. Baker, B. Bradley, and P. Stafford, *Seismic Hazard and Risk Analysis*. Cambridge University Press, 2021. doi: 10.1017/9781108425056.

J. Park, P. Bazzurro, and J. W. Baker, "Modeling spatial correlation of ground motion Intensity Measures for regional seismic hazard and portfolio loss estimation," *Applications of 838 Statistics and Probability in Civil Engineering*, pp. 1–8, 2007.

J. M. Rekoske, E. M. Thompson, M. P. Moschetti, M. G. Hearne, B. T. Aagaard, and G. A. Parker, "The 2019 Ridgecrest, California, Earthquake Sequence Ground Motions: Processed Records and Derived Intensity Metrics," *Seismological Research Letters*, vol. 91, no. 4, pp. 2010–2023, July 2020, doi: 10.1785/0220190292.

K. Goda and H. P. Hong, "Spatial Correlation of Peak Ground Motions and Response Spectra," *Bulletin of the Seismological Society of America*, vol. 98, no. 1, pp. 354–365, Feb. 2008, doi: 10.1785/0120070078.

L. Bodenmann, J. W. Baker, and B. Stojadinović, "Accounting for path and site effects in spatial ground-motion correlation models using Bayesian inference," *Natural Hazards and Earth System Sciences*, vol. 23, no. 7, pp. 2387–2402, July 2023, doi: 10.5194/nhess-23-2387-2023.

L. Eads, E. Miranda, and D. G. Lignos, "Average spectral acceleration as an intensity measure for collapse risk assessment," *Earthq Eng Struct Dyn*, vol. 44, no. 12, pp. 2057–2073, Sept. 2015, doi: 10.1002/eqe.2575.

L. Luzi, S. Hailemikael, D. Bindi, F. Pacor, F. Mele, and F. Sabetta, "ITACA (ITalian ACcelerometric Archive): A Web Portal for the Dissemination of Italian Strong-motion Data," *Seismological Research Letters*, vol. 79, no. 5, pp. 716–722, Sept. 2008, doi: 10.1785/gssrl.79.5.716.

M. Abbasnejadfard, M. Bastami, and A. Fallah, "Investigation of anisotropic spatial correlations of intra-event residuals of multiple earthquake intensity measures using latent dimensions method," *Geophys J Int*, vol. 222, no. 2, pp. 1449–1469, Aug. 2020, doi: 10.1093/gji/ggaa255.

M. Markhvida, L. Ceferino, and J. W. Baker, "Modeling spatially correlated spectral accelerations at multiple periods using principal component analysis and geostatistics," *Earthq Eng Struct Dyn*, vol. 47, no. 5, pp. 1107–1123, Apr. 2018, doi: 10.1002/eqe.3007.

M. Pagani *et al.*, "OpenQuake Engine: An Open Hazard (and Risk) Software for the Global Earthquake Model," *Seismological Research Letters*, vol. 85, no. 3, pp. 692–702, May 2014, doi: 10.1785/0220130087.

M. Wang and T. Takada, "Macrospatial Correlation Model of Seismic Ground Motions," *Earthquake Spectra*, vol. 21, no. 4, pp. 1137–1156, Nov. 2005, doi: 10.1193/1.2083887.

N. Jayaram and J. W. Baker, "Statistical tests of the joint distribution of spectral acceleration values," *Bulletin of the Seismological Society of America*, vol. 98, no. 5, pp. 2231–2243, Oct. 2008, doi: 10.1785/0120070208.

P. Heresi and E. Miranda, "Intensity Measures for Regional Seismic Risk Assessment of Low-Rise Wood-Frame Residential Construction," *Journal of Structural Engineering*, vol. 147, no. 1, Jan. 2021, doi: 10.1061/(ASCE)ST.1943-541X.0002859.

P. Heresi and E. Miranda, "RPBEE: Performance-based earthquake engineering on a regional scale," *Earthquake Spectra*, vol. 39, no. 3, pp. 1328–1351, Aug. 2023, doi: 10.1177/87552930231179491.

S. Akkar *et al.*, "Reference database for seismic ground-motion in Europe (RESORCE)," *Bulletin of Earthquake Engineering*, vol. 12, no. 1, pp. 311–339, Feb. 2014, doi: 10.1007/s10518-013-9506-8.

S. Aoi, T. Kunugi, and H. Fujiwara, "Strong-Motion Seismograph Network Operated by NIED: K-NET and KiK-net," *Journal of JAEE*, vol. 4, no. 3, pp. 65–74, 2004, doi: 10.5610/jaee.4.3_65.

S. Aristeidou, D. Shahnazaryan, and G. J. O'Reilly, "Artificial neural network-based ground motion model for next-generation seismic intensity measures," *Soil Dynamics and Earthquake Engineering*, vol. 184, p. 108851, Sept. 2024, doi: 10.1016/j.soildyn.2024.108851.

S. Aristeidou, D. Shahnazaryan, and G. J. O'Reilly, "Correlation models for next-generation amplitude and cumulative intensity measures using artificial neural networks," *Earthquake Spectra*, vol. 41, no. 1, pp. 851–875, Feb. 2025, doi: 10.1177/87552930241270563.

T. D. Ancheta *et al.*, "NGA-West2 Database," *Earthquake Spectra*, vol. 30, no. 3, pp. 989–1005, Aug. 2014, doi: 10.1193/070913EQS197M.

V. A. Monteiro & Gerard O'Reilly, "A review of ground motion correlation modelling for regional seismic risk analysis", Bulletin of Earthquake Engineering, 2026.

V. A. Monteiro & Gerard O'Reilly, "Notes on spatial correlation for average spectral acceleration: direct and indirect approaches", Earthquake Spectra, 2026.

W. Du and C.-L. Ning, "Modeling spatial cross-correlation of multiple ground motion intensity measures (SAs, PGA, PGV, Ia, CAV, and significant durations) based on principal component and geostatistical analyses," *Earthquake Spectra*, vol. 37, no. 1, pp. 486–504, Feb. 2021, doi: 10.1177/8755293020952442.